J Appl Physiol 102: 2227–2231, 2007.
First published February 1, 2007; doi:10.1152/japplphysiol.01137.2006.

Microchambers and macrochambers in heel pads: are they functionally different?

Chih-Chin Hsu,[2] Wen-Chung Tsai,[3] Chung-Li Wang,[4] Sun-Hua Pao,[1] Yio-Wha Shau,[1] and Yu-Shuan Chuan[1]

[1]*Institute of Applied Mechanics, National Taiwan University, Industrial Technology Research Institute, Taipei;* [2]*Department of Physical Medicine and Rehabilitation, Chang Gung Memorial Hospital, Keelung, College of Medicine, Chang Gung University, Taoyuan;* [3]*Department of Physical Medicine and Rehabilitation, Chang Gung Memorial Hospital, Linkou, College of Medicine, Chang Gung University, Taoyuan; and* [4]*Department of Orthopedic Surgery, Angiogenesis Research Center, National Taiwan University Hospital, Taipei, Taiwan*

Submitted 9 October 2006; accepted in final form 30 January 2007

Hsu C-C, Tsai W-C, Wang C-L, Pao S-H, Shau Y-W, Chuan Y-S. Microchambers and macrochambers in heel pads: are they functionally different? *J Appl Physiol* 102: 2227–2231, 2007. First published February 1, 2007; doi:10.1152/japplphysiol.01137.2006.— The heel pad consists of a superficial microchamber layer and a deep macrochamber layer. This study highlights the different biomechanical behaviors between the microchamber and macrochamber layers using ultrasonography. The heel pad in each left foot of six healthy volunteers aged ~25 yr old was measured with a device consisting of a 10-MHz linear-array ultrasound transducer and a load cell. The testing heels were loaded on the ultrasound transducer with a loading velocity of ~0.5 cm/s and were withdrawn when the specified maximum stress (158 kPa) was reached. Unloaded tissue thickness, end-loaded thickness, deformation proportion, average deformation, and rebound rates and elastic modulus of the microchamber and macrochamber layers were assessed. The unloaded thickness of the microchamber layer was ~30% of the macrochamber layer. The microchamber layer also had significantly less unloaded thickness, end-loaded thickness, mean deformation rate, mean rebound rate, and deformation proportion than the macrochamber layer. A significant difference between the unloaded and end-loaded thickness in the macrochamber layer was observed. The average soft tissue deformation rate was significantly different from the rebound rate in the microchamber layer. A similar trend was detected in the macrochamber layer. The elastic modulus of the microchamber layer was 450 kPa (SD 240), which was nearly 10 times of that in the macrochamber layer. In conclusion, ultrasound can identify the heterogeneous tissue properties of the heel pad. The macrochamber layer responds to loading with large deformation, and the microchamber layer has a high degree of tissue stiffness.

THE HEEL PAD, located beneath the calcaneus, is subject to repeated load bearing and functions as an efficient shock absorber during walking. The heel pad contains organized fibrous compartments that retain the adipose tissue. The fibrous septa extending from the skin to the calcaneal perichondrium is organized into small chambers connecting directly with the inside of the subcutis and greater chambers situated deep in the small chamber stratum. Therefore the human heel pad is anatomically divided into a superficial microchamber and a deep macrochamber layers (4). Although different anatomies for the subcalcaneal fat pad have been addressed, the roles of the respective portion in the heel pad in walking have not been formerly reported.

There is increasing interest in measuring heel-pad mechanical properties because pathological changes may not possess detectable structural alteration but generally correlate with changes in tissue biomechanics. Tissue behavior provides not only information regarding the material itself but also indicates the presence of a disease (16). Several approaches, including a material testing machine (3, 15), the drop impact test (13), the ballistic pendulum test (1), roentgenography (17), an ultrasonic indentation probe (23), a three-dimensional indentation system (14), the method integrating contact pressure measurements and a fluoroscopy (7), and an ultrasound-based loading-unloading device (10, 11, 22), have been utilized to study the heel-pad mechanical properties.

Tissue stiffness and dissipated energy for healthy and diseased heels have been described in these above studies. The heel pad was hypothesized as a single homogeneous material, which is in contrast to the inborn inhomogeneous nature of human soft tissues. Spears and Miller-Young (19) investigated the effect of heel-pad thickness (i.e., skinned and skinless) on heel-pad stiffness of cadaveric feet using material testing machine. As in vivo description of mechanical properties in each layer is limited, little is known about the function of microchamber and macrochamber layers in the heel pad. Further investigation is warranted to enhance knowledge of the different heel-pad anatomic layers. Findings may assist in preventing and treating shock-induced heel problems.

Understanding of heel-pad biomechanics can possibly be achieved with high-resolution ultrasonography, as this modality is versatile in diagnosing soft tissue pathologies in different locations (16) and has long been a reliable tool in assessing human heel-pad thickness (8, 18). This investigation attempted to obtain information associated with respective tissue displacement and biomechanical behaviors of the microchamber and macrochamber layers in the human heel pad.

MATERIALS AND METHODS

Six healthy volunteers, including four men and two women, were recruited in this study. Subject mean age was 25.2 yr (SD 0.98) (range: 24–27 yr). Mean body mass index was 21.6 kg/m^2

Address for reprint requests and other correspondence: Yio-Wha Shau, National Taiwan Univ. Industrial Technology Research Institute, No. 1, Roosevelt Rd., Sec. 4, Taipei 106, Taiwan (e-mail: shau0014@itri.org.tw).

The costs of publication of this article were defrayed in part by the payment of page charges. The article must therefore be hereby marked "*advertisement*" in accordance with 18 U.S.C. Section 1734 solely to indicate this fact.

(SD 1.6). No subjects had a foot problem within the last 6 mo before this study. A 10-MHz linear-array ultrasound transducer (HDI5000, Advanced Technology Laboratory, Bothell, WA) with a diameter of 39.7 mm was used to continually monitor the test heels. The transducer was incorporated into a Plexiglas cylinder and a contact surface area of 1.24×10^{-3} m^2. A load cell (U9B, HBM, Darmstadt, Germany) was on the bottom of the Plexiglas cylinder. Both the transducer and the load cell were then placed in a standing platform. When the transducer was loaded, force signals were transmitted to an amplifier (INA128/UAF42, Texas Instruments, Austin, TX) and then to a low-pass filter where frequencies above 10 Hz were filtered, by which the electronic noise and irrelevant motion artifacts were removed. The force signals were further transformed into stress data by dividing by the contact area during the assessment. The processed information was digitized using an analog-to-digital converter (DAQPad-6015, National Instruments) and then transmitted to an IBM-compatible personal computer. A pulse generator (Texas Instruments, Dallas, TX) was used to synchronize load cell signals and tissue thickness information. Figure 1 presents the experimental design. All subjects gave written informed consent before this noninvasive examination, and the ethics committee approved this study (Chang Gung Memorial Hospital Institutional Review Board 95-0095B).

Each left heel was pretreated with alcohol to allow the ultrasound to penetrate the soft tissue before the examination. A sufficient amount of jelly was applied to the transducer to enhance contact between the transducer and the tested heel. The subject then stood on the platform with the test heel on the ultrasound transducer and the other leg on the other platform; the platform height was approximately at the same level as the platform containing the ultrasound transducer. A cross sign was marked on the platform to identify the position of the built-in ultrasound transducer. The subject placed his or her foot axis, the line connecting the midheel and the second toe ray, along the indicated line. Then the subject loaded and unloaded the transducer rhythmically according to the metronome (quartz metronome SQ-77, Seiko S-Yard, Tokyo, Japan) frequency of 0.5 Hz. The subject loaded the transducer progressively from zero to maximum loading force of 196 N (maximum stress of 158 kPa). When this maximum value of loading force was reached, the system beeped, and the subject then withdrew his or her heel immediately. A loading-unloading cycle was completed when the heel was totally moved away from the ultrasound transducer. Average loading rate was calculated using the maximum deformation of the overall heel pad divided by the loading time interval (21). Average loading rate corresponding to the metronome frequency in this study was 0.52 cm/s (SD 0.13) (range 0.40–0.73 cm/s). Figure 2 presents ultrasound images for an unloaded, end-loaded, and fully relaxed heel pad.

The loading-unloading process of the heel pad was continuously monitored for 2 s by the ultrasound. The two-dimensional motion image was further divided into 90 frames of brightness mode pictures at successive time sequence in the loading-unloading cycle. The axial component of the strain image was estimated by comparing the gradient displacement between two successive pictures occurring after starting the examination. The unloaded thickness (Th_{unload}) and thickness measured at the maximum stress (Th_{max}) of the microchamber and macrochamber layers were determined by the echo tracking technique, respectively. The time-deformation curve for each layer was plotted according to the continuous ultrasound images (Fig. 3). Maximum deformation of the microchamber (ΔX_{mic}) was calculated as $\Delta X_{mic} = Th_{unload} - Th_{max}$. Maximum deformation of the macrochamber (ΔX_{mac}) was

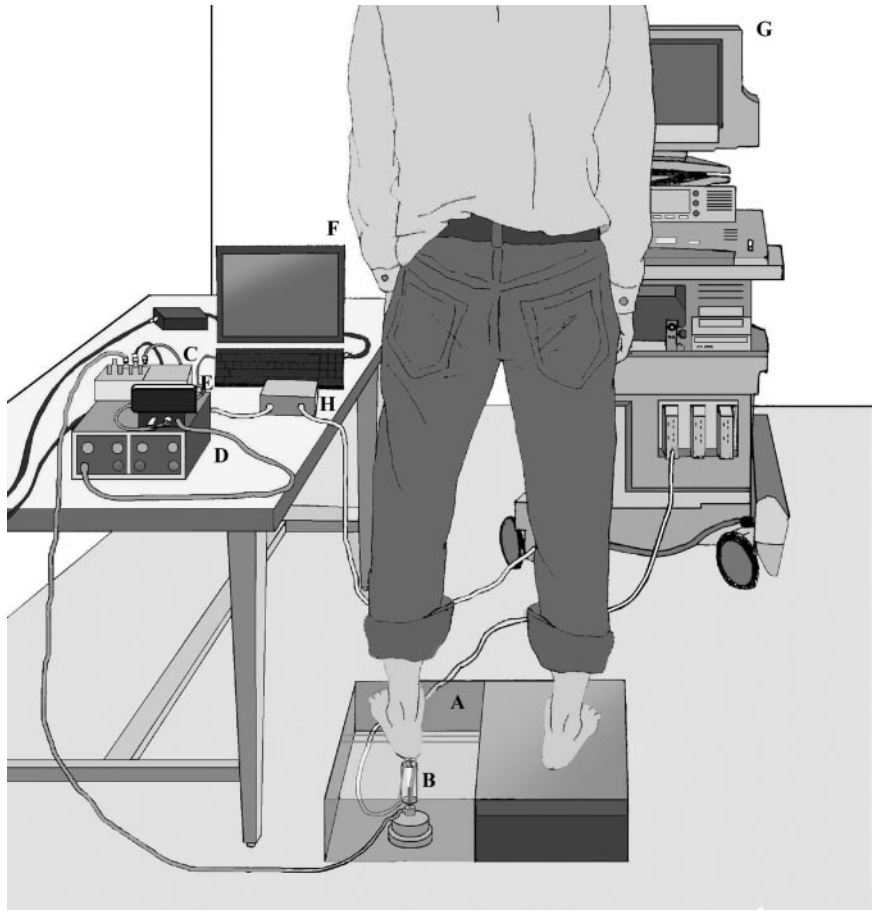

Fig. 1. Experimental design. The subject stood on a platform (A) with the test heel on the Plexiglas in which a 10-MHz compact linear array was embedded (B). The force signal of the loading-unloading process was transmitted to an amplifier (C) and then to a wall filter (D). The processed information was digitized by an analog-to-digital converter (E) and was then transmitted to an IBM-compatible personal computer (F). The dynamic image for the heel pad during the loading-unloading process was recorded by the ultrasound machine (G). A pulse generator (H) was used to synchronize force and deformation data.

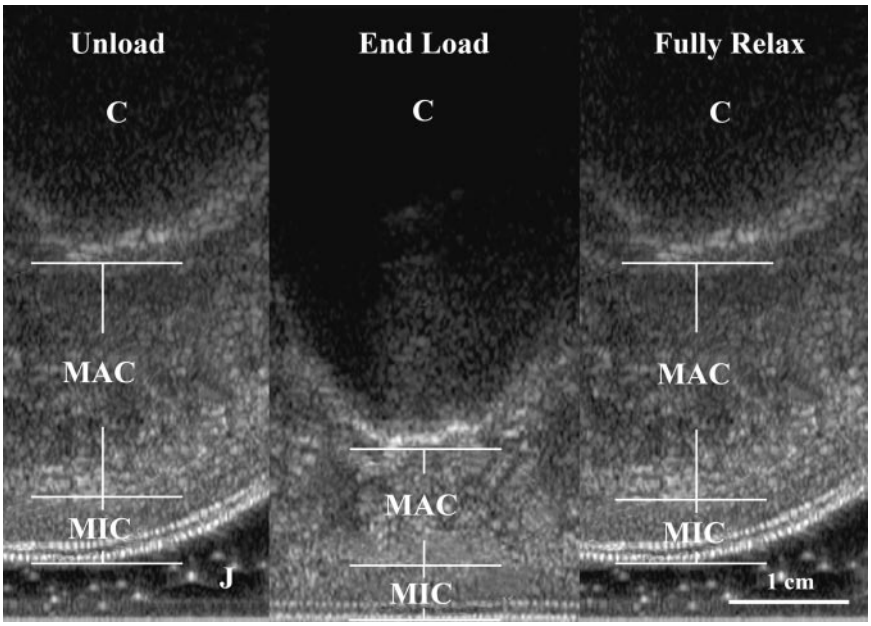

Fig. 2. Ultrasound image for the sagittal section, along the line connecting the midheel and the second toe ray of the heel pad underneath the calcaneus (C), in a 24-yr-old male subject while standing. *Left*, *middle*, and *right*: unloaded, end-loaded, and fully relaxed heel-pad conditions, respectively. An adequate amount of jelly (J) was placed between the test heel and the transducer during the examination. The microchamber (MIC) and macrochamber (MAC) layers in the heel pad can be easily identified ultrasonographically.

determined in the same manner. The proportion of maximum microchamber tissue deformation to the maximum overall heel-pad deformation was defined as $\Delta X_{mic}/(\Delta X_{mic} + \Delta X_{mac})$, and the proportion of maximum macrochamber tissue deformation to the maximum overall heel-pad deformation was defined as $\Delta X_{mac}/(\Delta X_{mic} + \Delta X_{mac})$. The maximum deformation ratio demonstrated the contribution of deformation of each layer during the examination. Average deformation rates for the microchamber and macrochamber layers at the loading (Def_{load}) and unloading (Reb_{unload}) phases were calculated from the time-deformation relationship and were defined as follows:

$$Def_{load} = \frac{\Delta X_{mic}}{T_{load}} \text{ (cm/s)} \quad \text{or} \quad Def_{load} = \frac{\Delta X_{mac}}{T_{load}} \text{ (cm/s)}$$

$$Reb_{unload} = \frac{\Delta X_{mic}}{T_{unload}} \text{ (cm/s)} \quad \text{or} \quad Reb_{unload} = \frac{\Delta X_{mac}}{T_{unload}} \text{ (cm/s)}$$

where T_{load} and T_{unload} represented loading and unloading periods, respectively, in the microchamber and macrochamber. The relationship between stress (σ) and strain (ϵ) of a elastic material could be described as $\sigma = E\epsilon$ (6). The elastic modulus (E), representing tissue stiffness, could be defined as:

$$E = \frac{P_{max}}{\left(\frac{Th_{unload} - Th_{max}}{Th_{unload}}\right)} \text{ kPa}$$

where P_{max} represents maximum stress, i.e., 158 kPa in this study.

Reliability was determined by a test-retest procedure. We repeated the measurement on the heel pad in five healthy individuals at intervals of 10 min, 2 h, and 1 wk after the first examination. The coefficient of variance for the assessment of unloaded thickness and E in the two layers ranged from 1 to 3% and 2.7% to 13.6%, respectively. Unloaded thickness, end-loaded thickness, deformation proportion, deformation rates, rebound rates, and the tissue stiffness between the microchamber and macrochamber layers were assessed using the Mann-Whitney U-test. Analysis was also conducted to estimate the differences between the loading and unloading processes during the examination period, and average deformation rates and

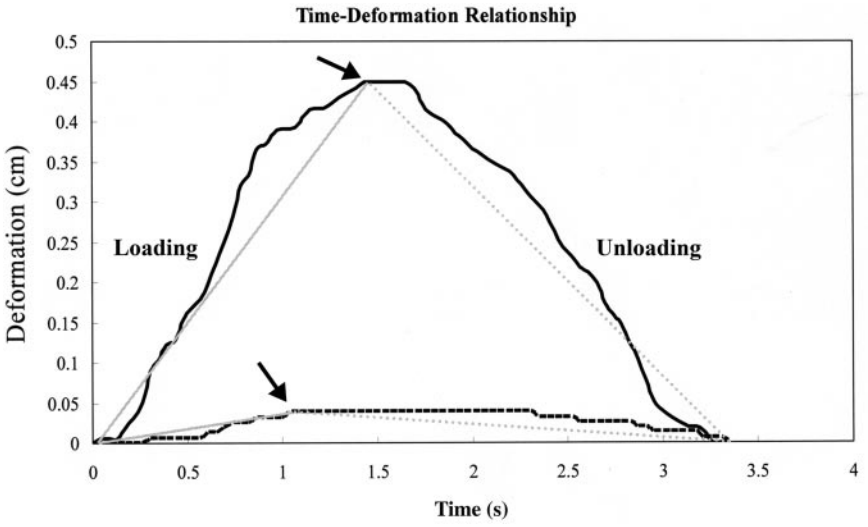

Fig. 3. Time-deformation curve for the left heel pad in a 27-yr-old male. The loading and unloading pathways of the macrochamber layer (solid black line) and the microchamber layer (dashed black line) are shown. The average deformation (solid gray line) and rebound (dashed gray line) rates for each layer were calculated from the beginning, the end-loaded (arrow), and the fully relaxed status.

average rebound rates within each layer. A value of $P < 0.05$ was considered statistically significant.

RESULTS

The mean values of unloaded thickness, end-loaded thickness, and elastic modulus for the heel pad between the skin and the calcaneus were 1.47 cm (SD 0.22), 0.88 cm (SD 0.08), and 50.7 kPa (SD 26), respectively. The tissue stiffness of the microchamber layer was significantly greater ($P = 0.002$) than that in the macrochamber layer. The microchamber layer also had significantly less unloaded thickness, end-loaded thickness, Def_{load}, Reb_{unload}, and deformation proportion than the macrochamber layer. A significant difference ($P = 0.002$) existed between average soft tissue deformation and rebound rates in the microchamber layer. Similar soft tissue responses during loading-unloading testing were detected in the macrochamber layer. The unloaded and end-loaded thickness were significantly different in the macrochamber layer. The loading and unloading intervals were similar between the two layers. Table 1 lists the detailed information for tissue properties in the microchamber and macrochamber layers.

DISCUSSION

Mechanical properties are determined primarily by the tissue composition (16). The fibrous septa within the human heel-pad contain predominantly elastic fibers in the thin microchamber layer and roughly an equal amount of collagen and elastic fibers in the thick macrochamber layer (5). Thus different biomechanical behaviors between the two subcutaneous compartments can be anticipated based on the different tissue compositions. In this study, high-resolution ultrasound identified unequal tissue displacement of various layers in the heel pad during loading-unloading examination. This novel observation indicates the anisotropic characteristics of the human heel pad, which may challenge the hypothesis that deformation is equally distributed in different heel-pad locations when receiving external disturbance. In this study, the bulk heel-pad tissue stiffness was close to macrochamber tissue stiffness because of greater volume effect and was considerably less than microchamber tissue properties. This finding has not been scientifically documented in the previous investigations.

Table 1. *Mechanical properties of the microchamber and macrochamber layers in the heel pad*

	Microchamber	Macrochamber	*P**
Unloaded thickness, cm	0.35 (0.08)	1.01 (0.18)	0.002
End-loaded thickness, cm	0.33 (0.08)	0.55 (0.15)	0.015
P†	0.818	0.004	
Examination duration, s			
Loading	1.37 (0.37)	1.40 (0.42)	0.699
Unloading	1.73 (0.34)	1.59 (0.28)	0.310
P†	0.754	0.884	
Deformation proportion × 100%	3.90 (1.8)	96.1 (1.8)	0.002
The tissue rate response in a loading-unloading cycle, cm/s			
Def_{load}	0.08 (0.03)	0.44 (0.10)	0.002
Reb_{unload}	0.045 (0.01)	0.37 (0.11)	0.002
P†	0.002	0.002	
E, kPa	450 (240)	46.4 (18)	0.002

Values are means (SD). *E,* elastic modulus; Def_{load}, average deformation rate for microchamber and macrochamber at the loading phase; Reb_{unload}, average deformation rate for microchamber and macrochamber at the unloading phase. *Mann-Whitney *U*-test for differences for among variables of unloaded thickness, end-loaded thickness, examination duration, deformation proportion, Def_{load}, Reb_{unload} and *E* between the microchamber and macrochamber layers. †Mann-Whitney *U*-test for differences between unloaded and end-loaded thickness, loading and unloading duration, Def_{load}, and Reb_{unload} during examination, respectively within each layer.

The unloaded human heel-pad thickness and its mechanical properties have been studied as altered tissue thickness, and biomechanical behaviors are proposed to have relationships with aging heels (11) and several shock-induced pathologies, including Achillodynia (12), heel pain syndrome (11), ulceration of the reconstructed musculocutaneous heel flap (22), and diabetic foot problems (10). The reported overall heel-pad thickness in healthy young persons is ~1.5 cm (11, 17, 23), and tissue stiffness in different age groups is approximately 40–300 kPa (3, 7, 10, 11). Different test devices (10), different test velocities (9), and heel geometry (19) can result in different tissue stiffness. Overall heel-pad tissue thickness and elastic modulus estimated in this study were located within previously reported ranges. However, tissue stiffness is quite different after dividing the heel pad into microchamber and macrochamber layers. In this study, the elastic modulus of the microchamber was ~10 times that in the macrochamber and was considerably higher than measured in any previous reports. The tendency agreed with findings based on recent finite element analysis for cadaveric heels (19).

In this study, the macrochamber layer was deformed immediately after compression and rebounded quickly after loading was removed. Under the same loading condition, the microchamber layer deformed faster, but the change in thickness is much less than the macrochamber layer. This observation is considered to be associated with the high tissue stiffness of microchambers. The different loading and unloading pathways, representing hysteresis of a viscoelastic material, within each layer and the different deformation behaviors between the two layers can be seen in the time-deformation curves (Fig. 3). These different physiological functions of the two anatomic layers in the human heel pad have not been previously identified. Obviously, the macrochamber layer plays a major role in the heel-pad tissue resiliency, i.e., the ability of the tissue to recover its shape after deformation caused by compression. This layer may be responsible for the cushioning effect in the heel pad during walking. The microchamber layer seems to function as an inherent heel cup that maintains most of the macrochamber layer beneath the calcaneus and prevents excessive macrochamber layer deformation.

Nonlinear heel-pad mechanical properties have been documented in many English literatures (2, 3, 10, 11, 13, 14). To provide more insight into the in vivo heel-pad heterogeneity, the stress and strain relationship in the study was based on the assumption of elastic materials, which could not simulate the nonlinear tissue behaviors. The stress in the macrochamber layer of the heel pad is equal to or less than the stress in the microchamber layer since the transducer is loaded on the superficial surface of the heel pad, and this may affect the quantification of tissue stiffness. More efforts are required to explore the nonlinear heel-pad tissue characteristics and stress inside a living soft tissue to achieve true heel-pad tissue nature.

In conclusion, the human heel pad is shown to be an inhomogeneous tissue in the study. The superficial microcham-

ber layer has greater tissue stiffness than the deep macrochamber layer. Substantial deformation of the macrochamber layer during loading-unloading examination was demonstrated. Different physiological functions in the two layers can be expected owing to the different biomechanics of the two layers. These findings may provide a treatment guide of injection of viscous supplement for reducing risk of tissue breakdown in diabetic patients (20). The therapeutic effects of interventions for different locations in the human heel pad can be monitored using the present technique.

ACKNOWLEDGMENTS

We thank our Department of Industrial Technology, Ministry of Economic Affairs, for hardware integration.

REFERENCES

1. **Aerts P, Ker RF, De Clerzq D, Ilsley SW.** The effects of isolation on the mechanics of the human heel pad. *J Anat* 188: 417–423, 1996.
2. **Basar Y, Itskov M.** Finite element formulation of the Ogden material model with application to rubber-like shells. *Int J Numer Methods Eng* 42: 1279–1308, 1998.
3. **Bennett MB, Ker RF.** The mechanical properties of the human subcalcaneal fat pad in compression. *J Anat* 171: 131–138, 1990.
4. **Blechschmidt E.** The structure of the calcaneal padding. *Foot Ankle* 2: 260–283, 1982.
5. **Buschmann WR, Jahss MH, Kummer F, Desai P, Gee RO, Ricci JL.** Histology and histomorphometric analysis of the normal and atrophic heel fat pad. *Foot Ankle Int* 16: 254–258, 1995.
6. **Fung YC.** *Biomechanics: Mechanical Properties of Living Tissues* (2nd ed). New York: Springer-Verlag, 1993.
7. **Gefen A, Megido-Ravid M, Itzchak Y.** In vivo biomechanical behavior of the human heel pad during the stance phase of gait. *J Biomech* 34: 1661–1665, 2001.
8. **Gooding GAW, Stress RM, Graf PM, Grunfeld C.** Heel pad thickness: determination by high-resolution ultrasonography. *J Ultrasound Med* 4: 173–174, 1985.
9. **Hsu CC, Tsai WC, Chen CPC, Shau YW, Wang CL, Chen MJL, Chang KJ.** Effects of aging on the plantar soft tissue properties under the metatarsal heads at different impact velocities. *Ultrasound Med Biol* 31: 1423–1429, 2005.
10. **Hsu TC, Wang CL, Shau YW, Tang FT, Li KL, Chen CY.** Altered heel-pad mechanical properties in type 2 diabetic patients. *Diabet Med* 17: 854–859, 2000.
11. **Hsu TC, Wang CL, Tsai WC, Kuo JK, Tang FT.** Comparison of the mechanical properties of the heel pad between young and elderly adults. *Arch Phys Med Rehabil* 79: 1101–1104, 1998.
12. **Jørgensen U.** Achillodynia and loss of heel pad shock absorbency. *Am J Sports Med* 13: 128–132, 1985.
13. **Kinoshita H, Francis PR, Murase T, Kawai S, Ogawa T.** The mechanical properties of the heel pad in elderly adults. *Eur J Appl Physiol* 43: 404–409, 1996.
14. **Klaesner JW, Hastings MK, Zou D, Lewis C, Mueller MJ.** Plantar tissue stiffness in patients with diabetes mellitus and peripheral neuropathy. *Arch Phys Med Rehabil* 83: 1796–1801, 2002.
15. **Miller-Young JE, Duncan NA, Baround G.** Mechanical properties of the human calcaneal fat pad in compression: experiment and theory. *J Biomech* 35: 1523–1531, 2002.
16. **Ophir J, Garra B, Kallel F, Konofagou E, Krouskop T, Righetti R, Varghese T.** Elastographic imaging. *Ultrasound Med Biol* 26, *Suppl* 1: S23–S29, 2000.
17. **Prichasuk PM, Mulpruek P, Siriwongpairat P.** The heel-pad compressibility. *Clin Orthop Relat Res* 300: 197–200, 1994.
18. **Rome K, Campbell R, Flint A, Haslock I.** Reliability of weight-bearing heel pad thickness measurements by ultrasound. *Clin Biomech* 13: 374–375, 1998.
19. **Spears IR, Miller-Young JE**. The effect of heel-pad thickness and loading protocol on measured heel-pad stiffness and a standardized protocol for inter-subject comparability. *Clin Biomech* 21: 204–212, 2006.
20. **Van Schie CH, Whalley A, Vileikyte L, Wignall T, Hollis S, Boulton AJM.** Efficacy of injected liquid silicone in the diabetic foot to reduce risk factors for ulceration: a randomized double-blind placebo-controlled trial. *Diabetes Care* 23: 634–638, 2000.
21. **Wang CL, Hsu TC, Shau YW, Shieh JY, Hsu KH.** Ultrasonographic measurement of the mechanical properties of the sole under the metatarsal heads. *J Orthop Res* 17: 709–713, 1999.
22. **Wang CL, Shau YW, Hsu TC, Chen HC, Chien SH.** Mechanical properties of heel pads reconstructed with flaps. *J Bone Joint Surg* [*Br*] 81B: 207–211, 1999.
23. **Zheng YP, Choi YKC, Wong K, Chan S, Mak AFT.** Biomechanical assessment of plantar foot tissue in diabetic patients using an ultrasound indentation system. *Ultrasound Med Biol* 26: 451–456, 2000.